Self-Assembled Nanotubes

DOI: 10.1002/anie.201001078

Metal–Organic Calixarene Nanotubes**

Stuart Kennedy, Georgios Karotsis, Christine M. Beavers, Simon J. Teat, Euan K. Brechin, and Scott J. Dalgarno**

The controlled assembly of molecular building blocks into nanoscale architectures is a fundamental challenge in supramolecular chemistry. Calix[4]arenes are cyclic and typically bowl-shaped molecules, some of which have been used to form large self-assembled molecular nanocapsules (NCs)[1] and nanotubes (NTs),[2] the latter of which are comparatively rare. In a small number of these studies it has been shown that variation of the crystallization conditions can induce either capsule or nanotubule formation depending on the co-crystallized species present (other than solvent).[1b,2d,g] Notably, Atwood and co-workers showed that combination of *p*-sulfonatocalix[4]arene (**1**) with lanthanum and pyridine-*N*-oxide (PNO) affords a coordination "C-shaped dimer" (Figure 1 A).[1b] The dimer possesses enough curvature to allow it to act as a versatile building block, capable of linking NCs or NTs (Figure 1 A), the centers of which contain water, and hydrated lanthanum and sodium ions that are coordinated to calixarene lower rims.

We have been interested in the controlled self-assembly of the *p*-carboxylatocalix[4]arenes, and have demonstrated the formation of various structural motifs when these molecules are crystallized from pyridine (Py) by varying the degree of lower-rim alkylation.[2h,j,3] Crystallization of **2** (Figure 1 B) from Py results in the formation of hexameric calixarene rings that interlock to form infinite hydrogen-bonded nanotubes.[2h] Pyridine molecules occupy the calixarene cavities and hydrogen bond with upper-rim carboxylic acid groups from neighboring nanotubes. Di-*O*-alkylation at the lower rim, and subsequent upper-rim alteration, affords tris-carboxylic acid **3** (Figure 1 C) that assembles into a triply helical nanotube when crystallized from Py.[2j] Similar H-bonding

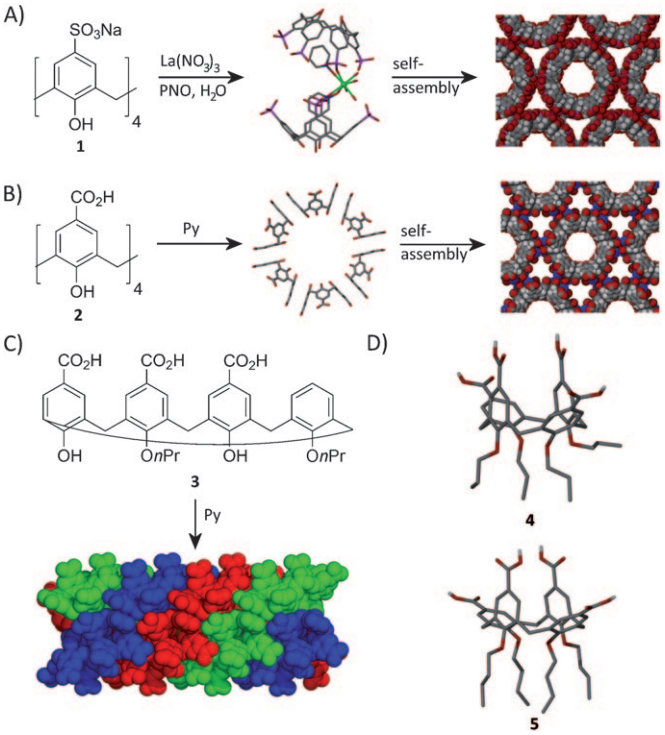

Figure 1. A) Assembly of **1** into a "C-shaped" dimer/nanotube.[1b] B) Assembly of **2** into discs/non-covalent nanotubes bridged by H-bonding interactions with Py (blue).[2h] C) Assembly of **3** into triply helical H-bonded nanotubes.[2j] D) Pinched cone **4** and **5**.[3] Nanotubes in (A) and (B) are viewed down the center of the tubules, while (C) shows the side view of a triply helical nanotube.

interactions are observed between cavity-bound Py molecules and neighboring nanotubes. Tetra-*O*-alkylation and upper-rim alteration to afford either **4** or **5** results in distortion of the molecular skeleton to afford pinched cone calixarene conformers (Figure 1 D).[3] Crystallization of **4** or **5** from Py results in a) exclusion of solvent molecules from the calixarene cavities due to conformational distortion, and b) two proximate upper-rim CO_2H groups.

We have demonstrated a high degree of control over nanotube/structure formation with these molecules, and we are interested in the formation of metal–organic structures as these would potentially offer enhanced stability within the resulting architectures and controlled bridging in nanometre scale assemblies. As a starting point we sought to form a discrete complex with a degree of curvature that may act as a linker for nanotube or nanocapsule arrays by forcing the molecules to pack in a back-to-back fashion rather than in antiparallel bilayer arrays. A search for transition metal (TM)

[*] S. Kennedy, Dr. S. J. Dalgarno
School of Engineering and Physical Sciences, Heriot-Watt University
Riccarton, Edinburgh, EH14 4AS (UK)
Fax: (+44) 131-451-3180
E-mail: S.J.Dalgarno@hw.ac.uk
G. Karotsis, Dr. E. K. Brechin
School of Chemistry, The University of Edinburgh
West Mains Road, Edinburgh, EH9 3JJ (UK)
Fax: (+44) 131-650-6453
E-mail: ebrechin@staffmail.ed.ac.uk
Dr. C. M. Beavers, Dr. S. J. Teat
Advanced Light Source, Berkeley Laboratory
1 Cyclotron Road, MS6R2100, Berkeley, CA 94720 (USA)

[**] The Advanced Light Source is supported by the Director, Office of Science, Office of Basic Energy Sciences, of the US Department of Energy under contract no. DE-AC02-05CH11231. We thank the EPSRC for financial support of this work.

Supporting information for this article is available on the WWW under http://dx.doi.org/10.1002/anie.201001078.

benzoate complexes in the Cambridge Structural Database returns many hits, a number of which suggested that the proximal nature of CO_2H groups in *p*-carboxylatocalix[4]arenes **4** and **5** could be utilized in the formation of discrete structures (linked by two TM centers) that would possess a degree of curvature to disturb bilayer formation.[4] Here, in our initial studies, we show that it is indeed possible to form discrete binuclear complexes, and that these do indeed pack into targeted self-assembled metal–organic nanotubes. This new nanotube motif contains three types of infinite solvent filled channels that differ in both shape and diameter.

It has been shown that the reaction of various TM salts with benzoic acids in the presence of N donor ligands (such as Py) results in the formation of binuclear aqua bridged complexes with the general formula $[TM_2(\mu\text{-}H_2O)(\mu\text{-}C_6H_5CO_2)_2(Py)_4(C_6H_5CO_2)_2]$ (Figure 2A).[4b] A survey of the crystal structures of these complexes shows a degree of variation in the arrangement of ligands around the metal coordination spheres relative to the bridging water molecule, as indicated by the arrows in the alternative view of $[Ni_2(\mu\text{-}H_2O)(\mu\text{-}C_6H_5CO_2)_2(Py)_4(C_6H_5CO_2)_2]$ in Figure 2A. We anticipated that the proximal nature of the CO_2H groups in **5** would result in slight reorientation of the Py ligands around the metal centers in analogous binuclear TM clusters. This would therefore result in the introduction of a degree of curvature to the resulting complex when considering the necessary positions of the calixarene subunits and the geometry of the metal centers. The curvature present in these complexes was predicted to render them less likely to pack in antiparallel bilayer arrays (that are common for *p*-substituted calixarenes), with the ultimate goal of promoting nanotube or nanocapsule formation by invoking back-to-back calixarene packing. In exploratory studies into this complex formation, methanolic Ni^{II} nitrate, Mn^{II} nitrate, or Co^{II} nitrate hydrates were added to methanol suspensions of **5**. Subsequent dropwise addition of pyridine was continued until dissolution of the suspension was achieved.[5] This resulted in a color change from green to blue for the Ni complex of **5**, and no color change for the analogous Mn and Co samples that remained pale yellow and pink, respectively. Crystals of the expected Ni, Co, and Mn complexes (**6**–**8**, respectively) were obtained by slow evaporation over a number of days; **6** formed as large blue blocks, whilst **7** and **8** formed as small pale pink or pale yellow needles, respectively, sharing a common unit cell. Single-crystal X-ray diffraction studies on **6**–**8** showed all three to be very weakly diffracting, and synchrotron radiation was required to obtain useful structural information for all.

Crystals of **6** are in a triclinic cell and structure solution was performed in the space group $P\bar{1}$.[6] The asymmetric unit is large, unexpectedly consisting of two discrete complexes (that show differences in ligand composition around the Ni centers; Figures 2B and S1 in the Supporting Information) and numerous disordered solvent molecules (Py, MeOH, and H_2O). The two complexes have formulas $[Ni_2(\mu\text{-}H_2O)(\mathbf{5})_2(Py)_4]$ and $[Ni_2(\mu\text{-}H_2O)(\mathbf{5})_2(Py)_3(MeOH)]$, and in both cases molecules of **5** act to replace the bridging and singly coordinating benzoates shown in Figure 2A. In both discrete complexes, the expected alteration to the metal coordination geometry has occurred, the result of which is that the calixarenes are arranged at an angle of around 150° to each other relative to a centroid generated between the two Ni centers (Figure S2). Although the introduction of curvature to the metal–organic assembly was successful, symmetry expansion shows the two complexes present in **6** to pack in bilayer type arrays (albeit with a degree of distortion) so that each layer is composed of either $[Ni_2(\mu\text{-}H_2O)(\mathbf{5})_2(Py)_4]$ or $[Ni_2(\mu\text{-}H_2O)(\mathbf{5})_2(Py)_3(MeOH)]$ (Figure S3).

Crystals of **7** are very weakly diffracting, are in a tetragonal cell, and structure solution was performed in the space group $I4_1/acd$.[6] The asymmetric unit comprises one half of a $[Co_2(\mu\text{-}H_2O)(\mathbf{5})_2(Py)_4]$ complex and disordered solvent molecules of crystallization (Py and H_2O). Notably there is no

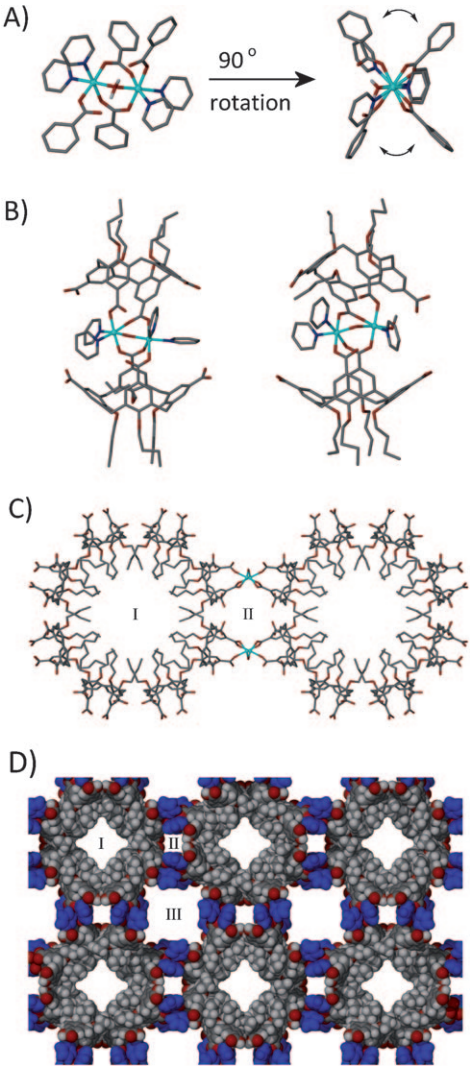

Figure 2. A) Orthogonal views of variable coordination spheres for TMs in $[TM_2(\mu\text{-}H_2O)(\mu\text{-}C_6H_5CO_2)_2(Py)_4(C_6H_5CO_2)_2]$ complexes, with arrows indicating flexibility in benzoate positioning. B) $[Ni_2(\mu\text{-}H_2O)(\mathbf{5})_2(Py)_4]$ and $[Ni_2(\mu\text{-}H_2O)(\mathbf{5})_2(Py)_3(MeOH)]$ complexes formed in this study. C) View down the center of the nanotubes in **7** showing bridging by $[Co_2(\mu\text{-}H_2O)(\mathbf{5})_2(Py)_4]$ building blocks and channels **I** and **II**. D) Space filling representation of the extended nanotube in **7** showing channels **I**–**III**. Ligated pyridines are shown in dark blue. Solvent molecules of crystallization are omitted for clarity.

$[Co_2(\mu\text{-}H_2O)(\mathbf{5})_2(Py)_3(MeOH)]$ present and this may be attributable to the fact that more Py was required to dissolve the precipitate during complex formation for **7** relative to **6**. Symmetry expansion of the asymmetric unit shows that when the coordination spheres of the Co centers are occupied by Py molecules, the discrete $[Co_2(\mu\text{-}H_2O)(\mathbf{5})_2(Py)_4]$ complexes pack in a remarkable nanotube structure that has a large internal solvent filled channel with a diameter of ca. 1.3 nm (channel **I**, Figure 2C, D).[7]

Within the extended structure of **7**, $[Co_2(\mu\text{-}H_2O)(\mathbf{5})_2(Py)_4]$ complexes act as bridges between neighboring nanotubes as we had anticipated (Figure 2C), and in doing so generate a small channel with a diameter of ca. 0.75 nm that is occupied by solvent of crystallization (channel **II**, Figure 2D and Figure S4). A further result of the way in which the discrete complexes pack is the generation of large square solvent filled channels (channel **III**, Figure 2D) that have a diameter of ca. 1.8 nm. The non-coordinating carboxylic acid groups on the calixarenes point into channels **II** and **III**, hydrogen bonding with solvent of crystallization. Interestingly the angle found between the calixarenes relative to a centroid generated between the two Co centers is 162°, which represents a large difference to that found in the crystal structure of **6**. Crystals of **8** are also very weakly diffracting, but have unit cell dimensions very similar to those of **7**, indicating that the two are isostructural.[6] As was the case for **7**, more Py was required for dissolution of the precipitate during complex formation for **8** relative to **6**. Unfortunately we were unable to obtain a meaningful data set to observe structural features for **8**.

Given the observation that more pyridine was required to form crystals of the targeted nanotube assembly in both **7** and **8**, we explored the addition of excess pyridine to a) crystals of **6**, and b) the reaction mixture following addition of methanolic Ni^{II} nitrate. In both cases crystals of **9** are formed by slow evaporation and these are found to have markedly different morphology relative to those of **6** (pale blue needles vs. blue blocks). The crystals of **9** are found to be very weakly diffracting to the point that it is not possible to obtain a unit cell even at long exposure. Comparison of X-ray powder diffraction patterns of **9** with a calculated pattern from **7** were inconclusive, and we attribute this to solvent loss upon crystal filtration. Although this is the case, we hypothesize that the formation of an isostructural nanotube or alternative structure containing curvature may be occurring under these conditions, thereby generating a material possessing highly disordered regions that inhibit diffraction and unit cell determination.

The variable-temperature magnetic behavior of **6**–**8**, measured using an applied field of 0.1 T, is plotted as the $\chi_m T$ product versus T (where χ_m is the molar magnetic susceptibility) in Figure 3. The room temperature $\chi_m T$ values of 2.7 (**6**) and 8.7 $cm^3 K mol^{-1}$ (**8**) are close to the values expected for two non-interacting $s = 1$ Ni^{2+} (2.4 $cm^3 K mol^{-1}$ for $g = 2.2$) and $s = 5/2$ Mn^{2+} (8.75 $cm^3 K mol^{-1}$ for $g = 2.0$) ions, respectively. As the temperature is decreased the value of $\chi_m T$ increases slowly for **6**, reaching a maximum value of 3.75 $cm^3 K mol^{-1}$ at 5 K. This is indicative of weak ferromagnetic exchange between the Ni^{2+} ions and an $S = 2$ ground state.[8] For **8** the value of $\chi_m T$ decreases slowly with temperature reaching a value of 3.2 $cm^3 K mol^{-1}$ at 5 K. This is suggestive of weak antiferromagnetic exchange between the metal centers and a diamagnetic ($S = 0$) ground state. The presence of two independent molecules in the unit cell of **6** with significantly different Ni–O(H_2O)–Ni bridging angles (113 and 115°) precludes successful simulation of the experimental data, but those for **8** can be satisfactorily simulated[9] with a simple isotropic 1J-model [$\mathscr{H} = -2J(S_1 S_2)$] affording the parameters $J = -1.0$ cm^{-1} and $g = 2.0$. This results in a diamagnetic ground state with several low-lying excited states.

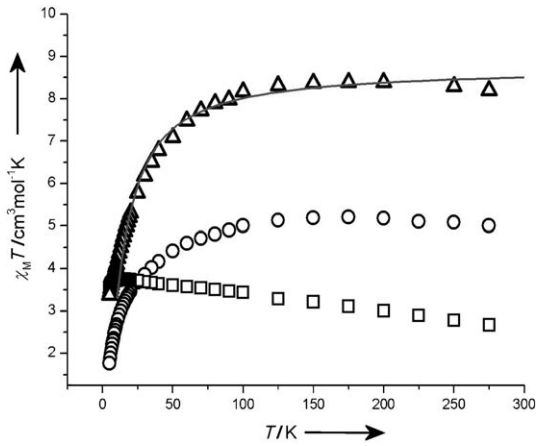

Figure 3. Plot of $\chi_m T$ versus T for **6** (□), **7** (○) and **8** (△) measured in an applied field of 0.1 T. The solid line is a simulation of the experimental data for **8**. See text for details.

The explanation of magnetic behavior of Co^{2+} complexes is complicated by the orbitally degenerate ground state of the ion and so precise derivation of the magnitude of the exchange interactions between cobalt centers is non-trivial. Therefore only a qualitative report of the magnetic susceptibility data for **7** follows. The room temperature $\chi_m T$ value of ca. 5.0 $cm^3 K mol^{-1}$ is consistent with the presence of two $s = 3/2$ ions with a g-value of 2.3. As the temperature is decreased the value of $\chi_m T$ increases very slowly to a maximum of 5.2 $cm^3 K mol^{-1}$ at 175 K, before decreasing below this temperature and reaching a value of 1.8 $cm^3 K mol^{-1}$ at 5 K.

To conclude, we have combined TM cluster formation and control over molecular conformation to demonstrate the targeted formation of novel self-assembled (magnetic) metal–organic nanotubes. The remarkable and general nanotube structure resulting from this study shows the presence of three different types of solvent filled channel. Solvent plays a pivotal role in altering the orientation of calixarenes around the cluster core, and there is vast scope for alteration of the channels in this new nanotube assembly by a) substitution at the lower rim of the calixarene skeleton, or b) the use of different pyridine or N-donor ligands for the TM centers. In addition, this nanotubular array has potential for either size selective guest exchange (depending on the channel selected) or multiple guest inclusion in different channels, and the inclusion of paramagnetic TMs in the assemblies opens up new perspectives in the field of supramolecular nanomagnet-

ism. Metal–organic nanotube formation with analogous complexes of **4**, structure alteration to the overall assembly, and studies into host–guest chemistry are currently underway.

Experimental Section

Compound **5** was synthesized according to literature procedures.[3] All other materials were purchased from Aldrich and used as supplied. Synthesis of **6:** Methanolic $Ni(NO_3)_2$ (104 mg, 0.36 mmol in 1 mL MeOH) was added to a suspension of compound **5** (70.5 mg, 0.086 mmol) in methanol. Following heating, the addition of pyridine (211 mg, 2.67 mmol) resulted in the green suspension changing to a homogeneous blue solution. Slow evaporation of the solvent over several days resulted in the near quantitative formation of blue block-shaped single crystals that were suitable for X-ray diffraction and magnetic studies. Synthesis of **7:** Methanolic $Co(NO_3)_2$ (103 mg, 0.35 mmol in 1 mL MeOH) was added to a suspension of compound **5** (70.7 mg, 0.086 mmol) in methanol. Following heating, the addition of pyridine (328 mg, 4.15 mmol) resulted in the red suspension changing to a homogeneous red solution. Slow evaporation of the solvent resulted in the near quantitative formation of red needle-shaped crystals that were suitable for X-ray diffraction and magnetic studies.

Synthesis of **8:** Methanolic $Mn(NO_3)_2$ (106 mg, 0.42 mmol in 1 mL MeOH) was added to a suspension of compound **5** (69.7 mg, 0.085 mmol) in methanol. Following heating, the addition of pyridine (309 mg, 3.91 mmol) resulted in the white suspension changing to a homogeneous colorless solution. Slow evaporation of the solvent resulted in the near quantitative formation of colorless needle-shaped crystals that were suitable for X-ray diffraction and magnetic studies. Synthesis of **9:** Crystals of **9** were obtained by two methods. Method 1: Methanolic $Ni(NO_3)_2$ (104 mg, 0.42 mmol in 1 mL MeOH) was added to a pyridine solution of **5** (71 mg, 0.086 mmol). Slow evaporation of the solvent from the resulting homogeneous blue solution resulted in the near quantitative formation of blue needle-shaped crystals. Method 2: Block-shaped crystals of **6** were harvested and dissolved in excess pyridine. Slow evaporation of the homogeneous blue solution resulted in the near quantitative formation of blue needle-shaped crystals. Microanalysis of freshly harvested crystals of **6**–**9** shows all to be solvent dependent, and as this was the case, TGA experiments were not performed.

Received: February 22, 2010
Revised: March 20, 2010
Published online: May 5, 2010

Keywords: calixarenes · magnetism · nanostructures · nanotubes · self-assembly

[1] For representative examples see: a) L. R. MacGillivray, J. L. Atwood, *Nature* **1997**, *389*, 469; b) G. W. Orr, L. J. Barbour, J. L. Atwood, *Science* **1999**, *285*, 1049; c) T. Gerkensmeier, W. Iwanek, C. Agena, R. Frölich, S. Kotila, C. Näther, J. Mattay, *Eur. J. Org. Chem.* **1999**, 2257; d) L. Avram, Y. Cohen, *J. Am. Chem. Soc.* **2002**, *124*, 15148; e) G. W. V. Cave, J. Antesberger, L. J. Barbour, R. M. McKinlay, J. L. Atwood, *Angew. Chem.* **2004**, *116*, 5375; *Angew. Chem. Int. Ed.* **2004**, *43*, 5263; f) L. Avram, Y. Cohen, *J. Am. Chem. Soc.* **2004**, *126*, 11556; g) J. L. Atwood, L. J. Barbour, S. J. Dalgarno, M. J. Hardie, C. L. Raston, H. R. Webb, *J. Am. Chem. Soc.* **2004**, *126*, 13170; h) S. J. Dalgarno, S. A. Tucker, D. B. Bassil, J. L. Atwood, *Science* **2005**, *309*, 2037; i) T. Evan-Salem, I. Baruch, L. Avram, Y. Cohen, L. C. Palmer, J. Rebek, Jr., *Proc. Natl. Acad. Sci. USA* **2006**, *103*, 12296; j) O. Ugono, K. T. Holman, *Chem. Commun.* **2006**, 2144; k) N. K. Beyeh, M. Kogej, A. Åhman, K. Rissanen, C. A. Schalley, *Angew. Chem.* **2006**, *118*, 5339; *Angew. Chem. Int. Ed.* **2006**, *45*, 5214; l) E. S. Barrett, T. J. Dale, J. Rebek, Jr., *J. Am. Chem. Soc.* **2007**, *129*, 3818; m) S. Yi, E. Milio, A. Kaifer, *Org. Lett.* **2009**, *11*, 5690.

[2] a) S. J. Coles, C. W. Hall, M. B. Hursthouse, *Acta Crystallogr. Sect. C* **2002**, *58*, o29; b) S. Stumpf, G. Goretzki, K. Gloe, K. Gloe, W. Seichter, E. Weber, J. W. Bats, *J. Inclusion Phenom. Macrocyclic Chem.* **2003**, *45*, 225; c) L. G. Kuz'mina, G. G. Sadikov, J. A. K. Howard, E. A. Shokova, V. V. Kovalev, *Kristallografiya* **2003**, *48*, 272; d) H. Mansikkamäki, M. Nissinen, K. Rissanen, *Angew. Chem.* **2004**, *116*, 1263; *Angew. Chem. Int. Ed.* **2004**, *43*, 1243; e) A. N. Lazar, N. Dupont, A. Navaza, A. W. Coleman, *Chem. Commun.* **2006**, 1076; f) F. Perret, A. D. Lazar, O. Shkurenko, K. Suwinska, N. Dupont, A. Navaza, A. W. Coleman, *CrystEngComm* **2006**, *8*, 890; g) S. J. Dalgarno, G. W. V. Cave, J. L. Atwood, *Angew. Chem.* **2006**, *118*, 584; *Angew. Chem. Int. Ed.* **2006**, *45*, 570; h) S. J. Dalgarno, J. E. Warren, J. Antesberger, T. E. Glass, J. L. Atwood, *New J. Chem.* **2007**, *31*, 1891; i) H. Dvořáková, J. Lang, J. Vlach, J. Sykora, M. Čajan, M. Himl, M. Pojarová, I. Stibor, P. Lhoták, *J. Org. Chem.* **2007**, *72*, 1675; j) S. Kennedy, S. J. Dalgarno, *Chem. Commun.* **2009**, 5275.

[3] S. Kennedy, S. J. Teat, S. J. Dalgarno, *Dalton Trans.* **2010**, *39*, 384.

[4] For example see: a) K. S. Hagen, R. Lachicotte, *J. Am. Chem. Soc.* **1992**, *114*, 8741 – 8742; b) A. Karmakar, R. J. Sarma, J. B. Baruah, *Eur. J. Inorg. Chem.* **2006**, 4673 – 4678; c) Y.-L. Shen, S.-L. Sun, W.-D. Song, *Acta Crystallogr. Sect. E* **2007**, *63*, m1309; d) S. Feng, *Acta Crystallogr. Sect. E* **2008**, *64*, m817; e) A. Karmakar, R. J. Sarma, J. B. Baruah, *Polyhedron* **2007**, *26*, 1347.

[5] Attempts to form the complexes directly from pyridine consistently resulted in the formation of the metal nitrate–pyridine clathrates. As this was the case, MeOH was used as an intermediary solvent.

[6] See Supporting Information for crystallographic details for **6**–**8**.

[7] There is severe disorder present in solvent molecules that occupy the channels formed by packing of the Co complex in **7**. Given this, the routine SQUEEZE was applied to remove the very diffuse electron density associated with these disordered molecules. This had the effect of strongly improving the agreement indices from $R_1 = 0.20$ to $R_1 = 0.1558$. A. L. Spek, *Acta Crystallogr. Sect. A* **1990**, *46*, C34.

[8] Magnetic studies on harvested crystals of **9** show them to behave in an analogous fashion to those of **6**. We assume that although small changes in the coordination environments on the Ni centers may influence the assembly of these moieties, the magnetic properties should be similar.

[9] J. J. Borrás-Alemnar, J. M. Clemente-Juan, E. Coronado, B. S. Tsukerblat, *J. Comput. Chem.* **2001**, *22*, 985.

